J Mater Sci: Mater Electron (2011) 22:1297–1302
DOI 10.1007/s10854-011-0303-3

The effect of nano sized $SrFe_{12}O_{19}$ additions on the magnetic properties of chromium-doped strontium-hexaferrite ceramics

Amir Abbas Nourbakhsh · Mohsen Noorbakhsh · Marzieh Nourbakhsh · Mehrdad Shaygan · Kenneth J. D. Mackenzie

Received: 12 December 2010 / Accepted: 17 January 2011 / Published online: 2 February 2011

Abstract Strontium hexaferrite ($SrFe_{12}O_{19}$) which crystallizes in the hexagonal system and has a uniaxial magnetoplumbite structure, displays distinctive magnetic characteristics, good chemical stability, good tribological properties and a weak temperature dependent coercivity at about room temperature. In the present work the synthesis conditions for the solid-state preparation of the chromium-doped hexaferrite $SrCr_{0.3}Fe_{11.7}O_{19}$ were optimised and the effect on the magnetic properties of this compound of additions of nanosized $SrFe_{12}O_{19}$ was studied. The nanosized $SrFe_{12}O_{19}$ additive, synthesized by the citrate–nitrate reaction, was substituted in varying amounts for a commercial calcium silicate borate sintering additive mixture. A combination of 0.75 wt% of nano-sized $SrFe_{12}O_{19}$ with 0.75 wt% of the commercial additive increases the intrinsic coercivity, remanence magnetization and rectangularity ratio and results in superior magnetic properties than obtained with 1.5 wt% of nanosized $SrFe_{12}O_{19}$ or the commercial sintering additive alone.

A. A. Nourbakhsh (✉) · M. Nourbakhsh · M. Shaygan
Ceramic Engineering Department, Islamic Azad University, Shahreza Branch, Isfahan, Iran
e-mail: anourbakhs@yahoo.com

M. Noorbakhsh
Taban Magnetic Material Development Co, Isfahan, Iran

K. J. D. Mackenzie
MacDiarmid Institute for Advanced Materials and Nanotechnology, Victoria University of Wellington, Wellington, New Zealand

1 Introduction

The hexagonal ferrites $MFe_{12}O_{19}$ (M = Ba, Sr, Pb) which have the magnetoplumbite structure (space group 63/mmc) are important permanent magnetic materials for microwave applications, small motors and magnetic recording applications [1]. Alabanese et al. [2] showed that in cationic-substituted M-type hexagonal ferrites the distribution of metallic ions among the different sub lattices is greatly modified by replacement of Ba with Sr . The permanent magnetic properties of hard ferrites are known to depend on their microstructural characteristics such as grain size, porosity, the presence of second phases and growth anisotropy [3]. High remanence requires a high sintered density and growth anisotropy, whereas high coercivity requires a small grain size [4]. Since the discovery of M-type hexagonal ferrites, extensive research has been carried out to improve their magnetic properties, particularly by the use of cationic substitutions [5, 6]. Some workers have substituted light rare-earth ions (LRE) such as La, Pr and other metal cations for Sr (Ba) and Fe respectively, taking into account of the ionic radius of elements [7].

Ba and Sr hexaferrites have been prepared by various techniques, including co-precipitation, the use of glass–ceramic or organic precursors, sol–gel synthesis, citrate–nitrate synthesis and ceramic processing [8–11]. Conventional solid state reactions for preparing barium and strontium ferrite powders require a high calcining temperature (1,200–1,300 °C) of milled mixtures of ferric oxide with barium or strontium carbonate. Furthermore, the milling process can introduce impurities into the material. Recently the sol–gel auto-combustion (citrate–nitrate) method has aroused interest because of its utilization of the heat released from the reactions of the hydrocarbon species from the

chelating agents with the nitrate oxidant, rapidly producing nano-powders in situ. The literature indicates that the use of nano powder improves the sintering ability of the system [12].

The present research determines the optimal conditions for the solid-state synthesis of chromium-doped $SrFe_{12}O_{19}$ and studies the influence on the magnetic properties of the resulting product of replacing the mixture of conventional sintering additives with varying amounts of nanosized strontium hexaferrite synthesized by the citrate–nitrate reaction.

2 Experimental

All the starting materials were of analytical grade, except the iron oxide which was rolling plant waste from the Mobareke Steel Company, Iran. The chemical analysis of this reactant is shown in Table 1.

Based on the composition of the iron oxide, the molar ratio of iron oxide to strontium oxide was taken as six. The oxides were blended in a polymer jar in a ball mill, using a ball: powder ratio of 11:1, milled at 550 rpm for 1 h. The optimal synthesis temperature required to obtain $SrFe_{12}O_{19}$ from this mixture was determined by heating samples in an electric furnace at a heating rate of 10 °C/min for 2 h at 1,140–1,220 °C. DTA patterns of this mixture (not shown here) suggest the formation of $SrFe_{12}O_{19}$ can occur at about 800 °C. The XRD patterns of the products were determined using a Brucker D8 diffractometer with Cu-Kα radiation and a Ni filter. The magnetic properties of all the samples were determined by measuring their hysteresis loops using a model AMT-4 magnetometer (Shuangji Electronic Co, China).

Samples of the $SrFe_{12}O_{19}$ prepared under the above optimised conditions were doped with varying amounts of Cr_2O_3 to produce a series of compounds $SrCr_xFe_{12-x}O_{19}$ where $x = 0 - 0.5$. Before firing these powder mixtures, 1.5 wt% of nano-sized $SrFe_{12}O_{19}$ prepared as described below was added as a sintering aid, and for comparison, some samples were prepared with 1.5 wt% of a commercial calcium silicate borate sintering aid (Type MN112, Taban Magnetic Material Development Co, Iran). Three types of samples were prepared, one containing only the commercial additive, one containing only the nano-sized $SrFe_{12}O_{19}$ and one containing 0.75 wt% of each additive. Aqueous slurries of these powder mixtures were blended in steel jars for 8 h with a ball: water: powder ratio of 11:3:1. The slurries were then pressed under a magnetic field of 400–800 A m^{-1} at a pressure of 100 MPa to form pellets 3 cm diameter × 1 cm high and fired in air at 1,210–1,260 °C for 2 h at a heating rate of 10°C/min.

The nano-sized $SrFe_{12}O_{19}$ sintering additive was synthesized by the sol–gel auto-combustion method [13]. $Fe(NO_3)_3.9H_2O$ and $Sr(NO_3)_2$ in the molar ratio 11.6:1 were dissolved in a minimum amount of deionised water. Citric acid was then added to chelate the Sr^{2+} and Fe^{3+} and the solution was brought to pH 7 by adding aqueous ammonia. The solution was evaporated to dryness by heating at 100 °C on a hot plate with continuous stirring until the mixture formed a viscous brown gel which was then calcined in air at different temperatures up to 1,100 °C for 1 h.

All the products were studied by XRD powder diffraction and SEM, after coating with Au, using a LEO 435 VP electron microscope operated at 20 keV. The B–H loops of all the samples were also determined.

3 Results and discussion

3.1 Optimization of the undoped $SrFe_{12}O_{19}$ synthesis temperature

The formation temperature of $SrFe_{12}O_{19}$ is related to the raw material characteristics such as their particle size, surface area and composition, as well as processing parameters such as the type of mixing. The XRD patterns of the present samples fired in the temperature range 1,180–1,210 °C were identical but differences were found in their magnetic properties. An increase in the calcination temperature from 1,180 to 1,210 °C results in an increase in the coercive field from 3,500 to about 4,000 Oe but the remanence and rectangularity ratio remains constant at about 3,600 G and 87%, respectively. Firing temperatures >1,210 °C result in partial sintering, making the samples difficult to mill for subsequent processing. Therefore, samples of $SrFe_{12}O_{19}$ for subsequent experiments were synthesised at 1,210 °C. The XRD pattern of undoped $SrFe_{12}O_{19}$ synthesised under these conditions at 1,210 °C is shown in Fig. 1.

3.2 Optimization of the $SrFe_{12}O_{19}$ sintering temperature

The magnetic properties of samples sintered with 1.5 wt% MN112 sintering additive at 1,210–1,260 °C show that

Table 1 Chemical analysis of iron oxide

Composition	Fe_2O_3	Cl	CaO	SiO_2	MnO	Al_2O_3	SO_3	MgO	ZnO	Cr_2O_3	CuO	K_2O	L.O.I	Total
Wt%	93.68	1.41	1.05	0.27	0.22	0.22	0.12	0.084	0.025	0.021	0.042	0.019	3.10	100.14

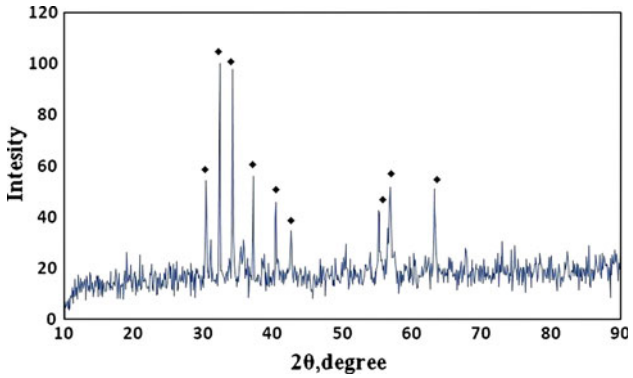

Fig. 1 XRD powder pattern of undoped $SrFe_{12}O_{19}$ powder fired at 1,210 °C. All peaks are from $SrFe_{12}O_{19}$ (JCPDS file no. 33-1340)

increasing the firing temperature produces an increase in the remanence magnetization from 3,975 to 4,130 G, due to increased sintering and decreased porosity. A concomitant decrease in coercive field from 3,518 to 2,882 Oe with increasing sintering temperature is probably related to increased grain growth. Since permanent-magnet applications require both high remanence and coercive field, these results led to the adoption of a sintering temperature of 1,220 °C for subsequent experiments on Cr-doped samples.

3.3 Optimization of the chromium dopant content

XRD patterns of Cr-doped $SrCr_xFe_{12-x}O_{19}$ samples where $x = 0-0.5$ (Fig. 2) show no change up to $x = 0.3$, but at $x = 0.5$ the non-magnetic hematite phase appears. Mossbauer studies [14] indicate that the hexagonal cell of $SrFe_{12}O_{19}$ contains five distinguishable crystallographic Fe sites, three octahedral 12k, $4f_2$ and 2a, one tetrahedral $4f_1$ and one bi- pyramidal 2b site. In general, Cr atoms do not occupy tetrahedral sites, ruling out substitution in the $4f_1$ site and confining the substitution to 10 of the 12 Fe^{3+} ions in $SrFe_{12}O_{19}$ [15].

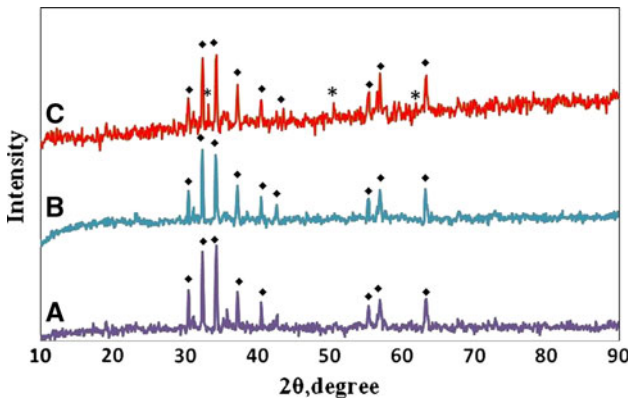

Fig. 2 XRD patterns of Cr-doped samples sintered at 1,220 °C with 1.5 wt% MN112 sintering additive. *a*. 0.1 atom % Cr, *B* 0.3 atom % Cr, *C* 0.5 atom % Cr. Peaks marked * are from hematite (JCPDS file no. 33-0664), all other peaks are from $SrFe_{12}O_{19}$ (JCPDS file no. 33-1340)

Since the ionic radii of Cr^{+3} and Fe^{+3} are almost equal, the appearance of hematite is unlikely to result from the effect of size but may be due to the change of exchange energy accompanying Cr^{3+} substitution in the lattice [15].

The magnetic properties of Cr-doped $SrCr_xFe_{12-x}O_{19}$ sintered at various temperatures in the presence of 1.5 wt% MN112 sintering additive are shown in Figs. 3 and 4 as a function of Cr content. Increasing the amount of chromium up to $x = 0.5$ results in a decrease of remanence magnetization at all temperatures (Fig. 3). This may be related to the electron configuration of Cr^{3+} which results in a magnetization of 3μB, whereas Fe^{3+} is 5μB. The presence of Cr^{3+} in $SrCr_xFe_{12-x}O_{19}$ can significantly affect the magnetic properties; it is reported that the total magnetic moment of $SrFe_{12}0_{19}$ in M-type hexaferrite is 20μB [16]. The magnetic saturation of the hexagonal ferrite lattice can be written [17]:

$$Ms = 6M^{Fe3+}_{(12K)} - 2M^{Fe3+}_{(4f2)} - 2M^{Fe3+}_{(4f1)} + M^{Fe3+}_{(2b)} + M^{Fe3+}_{(2a2)} \quad (1)$$

Under the most favourable conditions where the spins of Cr^{3+} and Fe^{3+} are aligned parallel in each site of the crystal structure, the magnetic saturation of the unit cell of chromium-doped hexaferrite is given by:

$$\begin{aligned} Ms = {} & [6(xM^{Fe3+}_{(12K)} + (1-x)\ M^{Cr3+}_{(12K)}] - 2[M^{Fe3+}_{(4f2)}) \\ & + (1-x)\ M^{Cr3+}_{(4f2)}] - 2M^{Fe3+}_{(4f1)} \\ & + [xM^{Fe3+}_{(2b)} + (1-x)\ M^{Cr3+}_{(2b)}] + [xM^{Fe3+}_{(2a2)} \\ & + (1-x)\ M^{Cr3+}_{(2a2)}] \end{aligned} \quad (2)$$

In the above equation, x is the mole fraction of crystal sites in the hexaferrite unit cell which are occupied by iron cations. According to above equation, it is evident that addition of chromium will decrease the remanence magnetization.

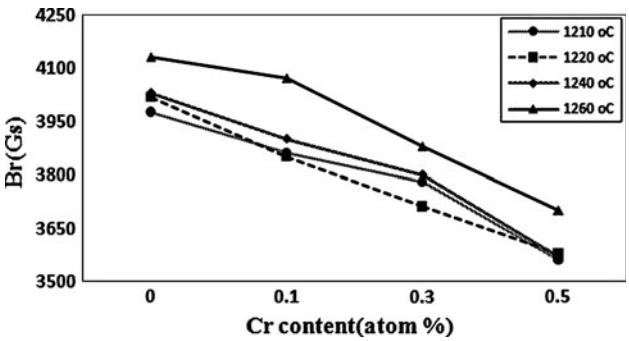

Fig. 3 Remanence magnetization of Cr-doped $SrFe_{12}O_{19}$ sintered with 1.5 wt% MN112 sintering additive as a function of Cr content

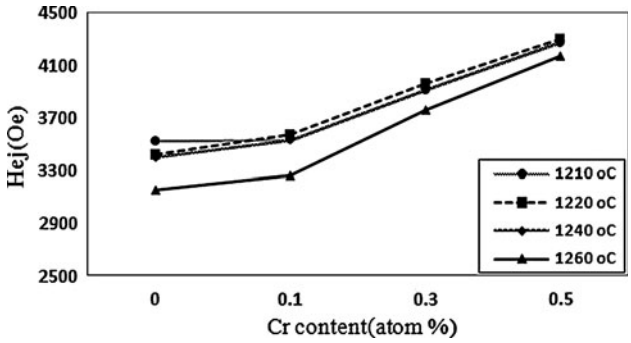

Fig. 4 Coercive field of Cr-doped $SrFe_{12}O_{19}$ sintered with 1.5 wt% MN112 sintering additive as a function of Cr content

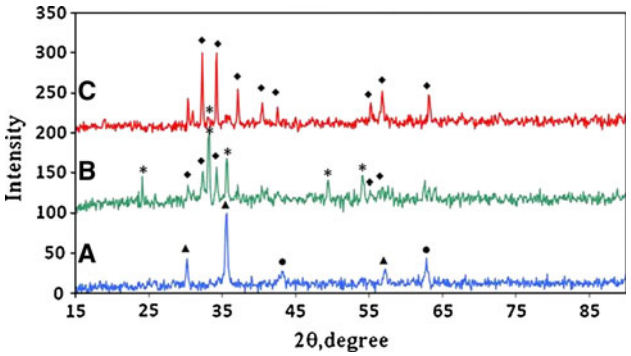

Fig. 5 XRD patterns of nano-sized $SrFe_{12}O_{19}$ prepared by the citrate–nitrate method. *a* as-synthesised, *b* calcined at 700 °C, *c* calcined at 1,100 °C. Peaks marked * are from hematite (JCPDS file no. 33-0664), peaks marked *filled diamond* are from $SrFe_{12}O_{19}$ (JCPDS file no. 33-1340), peaks marked *filled circle* are from maghemite (JCPDS file no. 39-1346) and peaks marked *filled triangle* are from magnetite (JCPDS file no.19-0629)

Figure 4 shows the intrinsic coercivity of Cr-doped samples sintered at various temperatures, as a function of the Cr concentration x up to $x = 0.5$. The addition of Cr up to $x = 0.5$ increases the intrinsic coercivity, as expected from Eq. 3 [18]

$$Hcj = \alpha(2K/Ms) \quad (3)$$

where Ms is the magnetic saturation and K is the magnetic anisotropy. According to Eq. 3, the addition of Cr will bring about a decrease in the remanence magnetization (Br) and saturation magnetization (Ms), causing an increase in the intrinsic coercivity.

These results suggest that a Cr doping content of $x = 0.3$ produces a product with optimal magnetic properties, and this composition was adopted for the subsequent studies of the effect of nano-sized $SrFe_{12}O_{19}$ additive.

3.4 Effect of nano-sized $SrFe_{12}O_{19}$ additions on the magnetic properties of $SrCr_{0.3}Fe_{11.7}O_{19}$

The synthesis of nano-sized $SrFe_{12}O_{19}$ powder by citrate–nitrate route is controlled by the ratio of Fe:Sr, the ratio of citrate to the other metal ions and the pH of the system. To obtain monophase $SrFe_{12}O_{19}$, the ratio of citrate ion to the metal ions was set at 1, with pH about 7 and a Fe:Sr ratio of 11.6:1. The XRD diffraction patterns of the unfired product and samples fired at 700 and 1,100 °C (Fig. 5) show that the optimal calcining temperature is 1,100 °C. At a higher Fe:Sr ratio of about 11.6:1, non-magnetic hematite appears.

The particle size of the nano-sized $SrFe_{12}O_{19}$ powder thus synthesized was calculated from the Scherrer Eq. 4 to be about 35 nm [15].

$$d(nm) = k\lambda/\beta\cos\theta \quad (4)$$

where λ is the X-ray wavelength, β is the half peak width, θ is the Bragg angle and k a constant, taken as 0.89. The high surface area and magnetic properties of this powder suggest that it should be a useful additive to enhance the magnetic properties of $SrFe_{12}O_{19}$ ceramics, and it was therefore used in the present studies on the $SrCr_{0.3}Fe_{11.7}O_{19}$ materials developed in the previous section, with and without the use of MN112 sintering additive.

Table 2 compares the magnetic properties of the initial $SrFe_{12}O_{19}$ powder, the sintered product doped with the optimal 0.3 mol Cr, and this doped material sintered with 1.5 wt% of nano-sized $SrFe_{12}O_{19}$, with the results for the sample containing 1.5 wt% sintering additive for comparison. Table 2 shows that sintering $SrCr_{0.3}Fe_{11.7}O_{19}$ with nano-sized $SrFe_{12}O_{19}$ additive alone produces little difference in remanence magnetization from the sample sintered without any additives, but the coercive field is

Table 2 Comparison of the magnetic properties of the various samples

Sample and firing temperature	Remanence magnetization (G)	Coercive field (Oe)	Rectangularity ratio (%)
Undoped $SrFe_{12}O_{19}$ powder (1,210 °C)	3,673	4,048	87.1
$SrCr_{0.3}Fe_{11.7}O_{19}$ (no additive, sintered 1,220 °C)	3,806	2,941	76.9
$SrCr_{0.3}Fe_{11.7}O_{19}$ +1.5 wt% nano- $SrFe_{12}O_{19}$ (sintered 1,220 °C)	3,888	2,525	91
$SrCr_{0.3}Fe_{11.7}O_{19}$ + 1.5 wt% MN112 (sintered 1,220 °C)	3,662	3,928	70
$SrCr_{0.3}Fe_{11.7}O_{19}$ + 0.75 wt% nano- $SrFe_{12}O_{19}$ + 0.75 wt% MN112 (sintered 1,220 °C)	3,687	4,129	84

significantly decreased by the presence of the nano-additive. The use of MN112 sintering additive decreases the remanence magnetization of undoped $SrCr_{0.3}Fe_{11.7}O_{19}$ but significantly increases the coercive field; this effect is even more pronounced in the sample containing equal proportions of MN112 and nano- $SrFe_{12}O_{19}$ (Table 2), indicating that this combination of additives produces the best practical magnetic material.

The reasons for these results can be seen from the SEM microstructures of these samples (Fig. 6). The sample containing only MN112 (Fig. 6b) is seen to be better

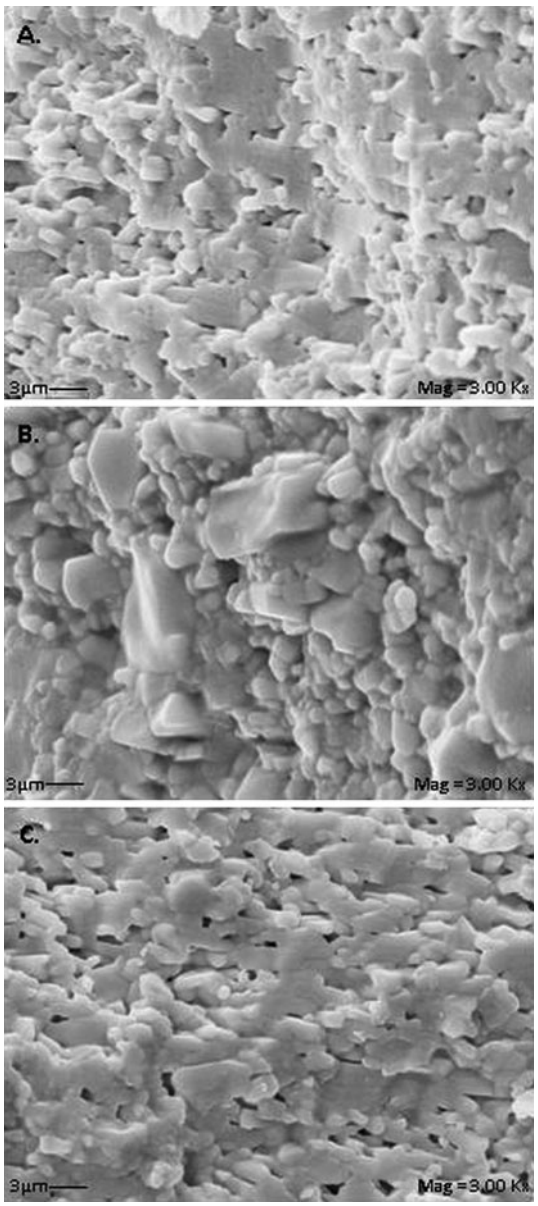

Fig. 6 SEM micrographs of $SrCr_{0.3}Fe_{11.7}O_{19}$ sintered at 1,220 °C, **a** with 1.5 wt% nano-sized $SrFe_{12}O_{19}$, **b** with 1.5 wt% MN112 sintering additive, **c** with 0.75 wt% nano-sized $SrFe_{12}O_{19}$ + 0.75 wt% MN112 sintering additive

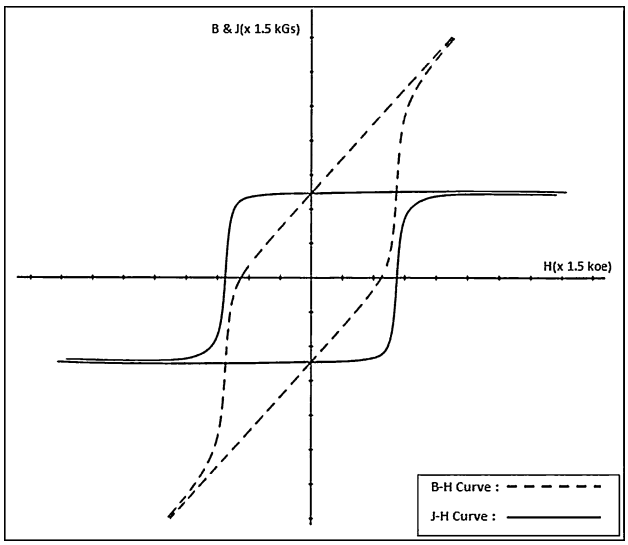

Fig. 7 Hysteresis loop of optimised $SrCr_{0.3}Fe_{11.7}O_{19}$ sample sintered at 1,220 °C with 0.75 wt% nano-sized $SrFe_{12}O_{19}$ + 0.75 wt% MN112 sintering additive

sintered than the sample containing only nano-sized $SrFe_{12}O_{19}$, which shows a greater degree of grain growth (Fig. 6a). This enhanced grain growth is the probable explanation for the decreased coercivity in this sample. Use of the two additives together combines the best properties of each, producing the sample with a superior coercive field and therefore the best magnetic properties for practical applications. The two hysteresis loops (B–H and J-H) of this optimized $SrCr_{0.3}Fe_{11.7}O_{19}$ sample sintered with a combination of 0.75 wt% MN112 sintering additive and 0.75 wt% nano-sized $SrFe_{12}O_{19}$ are shown in Fig. 7. The flux density (B) is the constant multiple of the magnetic field (H) added to the magnetization (J).So compared to the J-H loop, the B–H curve has a higher right shoulder.

4 Conclusions

Samples of $SrFe_{12}O_{19}$ were doped with 0.3 atom % Cr^{3+} and sintered with the addition of 1.5 wt% nano-sized $SrFe_{12}O_{19}$ in conjunction with a commercial calcium silicate borate sintering aid. The optimum conditions for the development of the magnetic properties of these samples was determined to be 1,220 °C with a 0.3 atom % Cr^{3+} content; higher Cr contents lead to the appearance of non-magnetic hematite. The addition of nano-sized $SrFe_{12}O_{19}$ alone leads to enhanced grain growth, with deleterious effects on the magnetic properties, particularly the important coercive field value, whereas the use of 1.5 wt% of commercial sintering additive alone promotes greater sintering with a significant enhancement of the coercive field. The combination of 0.75 wt% of each additive produces

the best magnetic properties in these Cr-doped samples (a remanence magnetization of 3,687 G, a coercive field of 4,129 Oe and a rectangularity ratio of 84%).

References

1. J.D. Liringgston, Jox, 42, (1990)
2. G. Albanese, M. Carbucicchio, A. Deriu, Nuovo Cimento **B15**, 147 (1973)
3. A. Singh, B. Narang, K. Singh, O.P. Pandey, R.K. Kotnala, J. Ceram. Proc. Res. **11**, 241 (2010)
4. S. Besebicar, M. Drfenik, J. Mag. Magn. Mater. **101**, 307 (1991)
5. E.P. Wohlfarth, *Handbook of Magnetic Material* (North-Holland, Amsterdam, 1982)
6. B.D. Cullity, *Introduction to Magnetic Materials* (Addison-Wesley, Massachusetts, 1972)
7. X. Liu, W. Zhong, S. Yang, Z. Yu, B. Gu, Phys. Stat. Sol. **193**, 314 (2002)
8. A. Ataei, S. Heshmati-Manesh, J. Eur. Ceram. Soc. **21**, 1951 (2001)
9. J.F. Wang, C.B. Paton, R. Ciossinger, I.R. Harris, J. Alloys Cpds. **369**, 170 (2004)
10. M. Mirkazemi, V.K. Marghusiiam, A. Beitollahi, Ceram. Int. **32**, 43 (2006)
11. L. Junliang, Z. Yanwei, C. Cuijing, Z. Wei, Y. Xiaowei, J. Eur. Ceram. Soc. **30**, 993 (2010)
12. W.D. Kingery, H.K. Bowen, D.R. Uhlmann, *Introduction to Ceramics* (Wiley, New York, 1976)
13. S. Chaudhury, S.K. Rakshit, S.C. Parida, Z. Singh, J. Alloys Cpds. **455**, 25 (2008)
14. P.M. Rao, G. Rard, P. Grandjea, Phys. Stat. Sol, **54**, 529 (1979)
15. Q. Fang, H. Cheng, K. Haung, J. Wang, R. Li, Y. Jiao, J. Mag. Magn. Mater. **294**, 281 (2005)
16. A. Goldman, *Modern Ferrite Technology* (Nostrand Reinhold, New York, 1990)
17. R.H. Arendtm, J. Appl. Phys. **44**, 3300 (1973)
18. C. Kittel, *Introduction to Solid State Physics* (Wiley, New York, 2005)